AD-A058 857 ILLINOIS UNIV AT URBANA-CHAMPAIGN DEPT OF ELECTRICAL --ETC F/G 9/4
DESIGN, ERROR ANALYSIS AND OPERATION OF A NOISE AUTOCORRELATOR.(U)
MAY 78 M J MCNUTT, C T SAH F19628-77-C-0138
UNCLASSIFIED SCIENTIFIC-2 RADC-TR-78-114 NL

1 OF 1
AD
A058 857

END
DATE
FILMED
-11-78
DDC

LEVEL II

RADC-TR-78-114
Interim Report
May 1978

DESIGN, ERROR ANALYSIS AND OPERATION OF A NOISE AUTOCORRELATOR

Michael J. McNutt
C. T. Sah

University of Illinois

Approved for public release; distribution unlimited.

ROME AIR DEVELOPMENT CENTER
Air Force Systems Command
Griffiss Air Force Base, New York 13441

This report has been reviewed by the RADC Information Office (OI) and is releasable to the National Technical Information Service (NTIS). At NTIS it will be releasable to the general public, including foreign nations.

RADC-TR-78-114 has been reviewed and is approved for publication.

APPROVED: Jerry Silverman

JERRY SILVERMAN
Project Engineering

APPROVED: Robert M Barrett

ROBERT M. BARRETT, Director
Solid State Sciences Division

FOR THE COMMANDER: John P. Huss

JOHN P. HUSS
Acting Chief, Plans Office

If your address has changed or if you wish to be removed from the RADC mailing list, or if the addressee is no longer employed by your organization, please notify RADC (ESE), Hanscom AFB MA 01730.

Do not return this copy. Retain or destroy.

UNCLASSIFIED

SECURITY CLASSIFICATION OF THIS PAGE (When Data Entered)

REPORT DOCUMENTATION PAGE

READ INSTRUCTIONS BEFORE COMPLETING FORM

1. REPORT NUMBER: RADC-TR-78-114	2. GOVT ACCESSION NO.
3. RECIPIENT'S CATALOG NUMBER	
4. TITLE (and Subtitle): DESIGN, ERROR ANALYSIS AND OPERATION OF A NOISE AUTOCORRELATOR	5. TYPE OF REPORT & PERIOD COVERED: Scientific Report, No. 2, 01OCT77 - 31MAR78
	6. PERFORMING ORG. REPORT NUMBER: C-0138-SR-2-TR-34
7. AUTHOR(s): Michael J. McNutt, C. T. Sah	8. CONTRACT OR GRANT NUMBER(s): F19628-77-C-0138
9. PERFORMING ORGANIZATION NAME AND ADDRESS: Department of Electrical Engineering, University of Illinois, Urbana, Illinois 61801	10. PROGRAM ELEMENT, PROJECT, TASK AREA & WORK UNIT NUMBERS: 61102F, 2306J226
11. CONTROLLING OFFICE NAME AND ADDRESS: Deputy for Electronic Technology (RADC), Hanscom AFB, Massachusetts 01731, Monitors/J. Silverman/ESE	12. REPORT DATE: MAY 1978
	13. NUMBER OF PAGES: 38
14. MONITORING AGENCY NAME & ADDRESS(if different from Controlling Office)	15. SECURITY CLASS. (of this report): UNCLASSIFIED
	15a. DECLASSIFICATION/DOWNGRADING SCHEDULE

16. DISTRIBUTION STATEMENT (of this Report)

Approved for public release; distribution unlimited

17. DISTRIBUTION STATEMENT (of the abstract entered in Block 20, if different from Report)

18. SUPPLEMENTARY NOTES

19. KEY WORDS (Continue on reverse side if necessary and identify by block number)

Autocorrelation	Charge Coupled Devices	Silicon
Hardware correlator	CCD	
Noise	MOSFET	
Software correlator	Semiconductors	

20. ABSTRACT (Continue on reverse side if necessary and identify by block number)

Low frequency 1/f noise limits the ultimate sensitivity of semiconductor devices such as MOSFET (MOS Field-Effect-Transistor) and CCD (Charge Coupled Devices). The study of the origin of the low frequency noise sources requires detailed measurements of the noise power spectra under a wide range of device operating conditions. This report details the design and operation of a hardwired noise correlation processor (correlator) which is interfaced to a host computer for two-way handshaking operation. The correlator samples the noise voltage from a device under study as well as calculates, averages and stores the

DD FORM 1 JAN 73 1473 EDITION OF 1 NOV 65 IS OBSOLETE

UNCLASSIFIED

SECURITY CLASSIFICATION OF THIS PAGE (When Data Entered)

20. ABSTRACT

autocorrelation function of the noise. The host computer can then sample the autocorrelation data, calculate the power spectrum and plot the results, all on a low priority time sharing basis if necessary. This system provides the flexibility of programmable control and the speed and accuracy of dedicated hardware correlator. In order to optimize the correlator design, a detailed analysis of sampling, correlation and noise theory were undertaken which provided some important insights on sampling quantization errors, and noise power averaging techniques using incomplete correlation. These theoretical concepts apply to a wide range of situations of signal correlation, as well as noise power spectra measurements on silicon semiconductor devices.

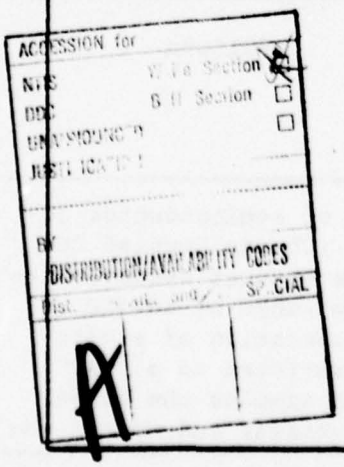

SUMMARY

Low frequency 1/f noise limits the ultimate sensitivity of semiconductor devices such as MOSFET (MOS Field-Effect-Transistor) and CCD (Charge Coupled Devices). The study of the origin of the low frequency noise sources requires detailed measurements of the noise power spectra under a wide range of device operating conditions. This report details the design and operation of a hardwired noise correlation processor (correlator) which is interfaced to a host computer for two-way handshaking operation. The correlator samples the noise voltage from a device under study as well as calculates, averages and stores the autocorrelation function of the noise. The host computer can then sample the autocorrelation data, calculate the power spectrum and plot the results, all on a low priority time sharing basis if necessary. This system provides the flexibility of programmable control and the speed and accuracy of dedicated hardware correlator. In order to optimize the correlator design, a detailed analysis of sampling, correlation and noise theory were undertaken which provided some important insights on sampling quantization errors, and noise power averaging techniques using incomplete correlation. These theoretical concepts apply to a wide range of situations of signal correlation, as well as noise power spectra measurements on silicon semiconductor devices.

TABLE OF CONTENTS

I. INTRODUCTION 1

II. SAMPLING THEORYEMS 2

III. NOISE SAMPLE TIME 9

IV. CORRELATION PROCEDURE 12

V. QUANTIZATION AND SAMPLING ERROR 21

VI. EXPERIMENTAL RESULTS 32

VII. CONCLUSION 36

REFERENCES 38

LIST OF FIGURES

Figure		Page
1	The time dependence and the frequency spectra of (a) a noise signal, (b) the impulse train and (c) the box function	3
2(a)	The software calculated autocorrelation function of a 0.2 Hz sine wave at two amplitudes	13
2(b)	The software calculated power spectra of a 0.2 Hz sine wave at two amplitudes	14
3	The percentage noise power variance as a function of the number of sample periods with incomplete correlation as a parameter	17
4	The calculation time as a function of the lowest frequency for complete and incomplete correlation using a desk calculator or a minicomputer	19
5	The box diagram of the hardware correlator	20
6	The noise voltage amplitude distribution function and its Fourier transform	22
7	The round-off function, ROUNDv, as a function of the normalized voltage v/h	24
8	The quantization error of the noise voltage, v, as a function of the average voltage	27
9	The quantization error of the noise power, v^2, as a function of the average voltage	28
10	The correlation coefficient of the quantization noise, ρ_{QN}, as a function of the correlation coefficient of the input noise voltage, ρ_N	30
11	Oscilloscope photographs of the correlator processed autocorrelation functions for (a) sinusoidal, (b) square wave, (c) white noise and (d) Lorentzian noise input signals. The input signals are shown in the lower part of each figure and the autocorrelation functions are shown in the upper part of each figure . . .	33
12	The autocorrelation function of a Lorentzian noise	35

Figure		Page
13	The power spectrum of the Lorentzian noise shown in Figure 12	36
14	The three-point smoothed power spectrum of the Lorentzian noise shown in Figure 13	37

DESIGN, ERROR ANALYSIS AND OPERATION OF A NOISE AUTOCORRELATOR

I. INTRODUCTION

In the research on the mechanisms of noise generation in solid state devices, the most time-consuming and tedious task is probably the manual experimental measurement of the noise power spectra, especially at low frequencies such as 1 or 10 Hz. Brute force approach for manual narrow band noise measurements is very time-consuming since meaningful results can be obtained only after averaging over a time interval substantially larger than the reciprocal bandwidth.

This report presents a theoretical analysis, design, and experimental implementation as well as operation of a computer-controlled automatic noise data acquisition system. The stored noise data in the computer memory can be analyzed further and presented in tabulated and graphic forms.

In designing a noise autocorrelator, it is important to study tradeoffs among hardware cost, speed, and accuracy. Some of the subjects covered in this report are generally applicable to all types of input signals for both hardware and software correlators. However, we are interested primarily in noise spectral analysis, and this will point ultimately to a hardware instrument. We will find that some of the design parameters are surprisingly noncritical, whereas others are extremely limiting. By examining the errors due to all the parameters, the most efficient combination can be put together. Very early, however, the decision was made to use digital rather than analog computation due to the inherent advantages in the frequency and dynamic range.

In the second chapter, the basic concepts of the Nyquist theorem, the autocorrelation function, and the Wiener-Khintchine theorem are briefly

discussed along with mention of analog-digital conversion errors. The third chapter investigates the sampling time required to obtain a good average of each of the noise signal's spectral components. This information is used in chapter four to choose between hardware and software correlation and between complete and incomplete data analysis schemes. The many samples, shown to be necessary by the analysis, allow the use of large input quantization errors while maintaining output accuracy, and determine the relative unimportance of the error due to a finite number of samples. This is discussed in chapter five. Finally, operation of the correlator is discussed in chapter six and is illustrated with sample correlator outputs and computer printouts.

II. SAMPLING THEOREMS

The modern sampling theorem is generally credited to Nyquist[1] and has been extended by Shannon[2]. This sampling or Nyquist theorem states that a function limited to frequencies where $|f|<f_0$ can be perfectly reproduced by sampling isolated points at a fixed frequency of $2f_0$ or greater. This theorem is somewhat idealized, however, and, in practice, errors are always present due to high frequency aliasing, limited frequency resolution, and finite sampling windows.

Sampling a time function at a fixed frequency, $2f_0$, is equivalent mathematically to multiplication of the function by an impulse train or convolution of the frequency spectrum by an impulse train. This results in reproducing the frequency spectrum at intervals of $2f_0$. As long as the spectrum is exactly zero for $|f|<f_0$, there is no overlap of the adjacent identical frequency spectra, and the original spectrum can be obtained by running the signal through a low pass filter or simply ignoring the $f>f_0$ components of the total calculated spectrum. This is depicted graphically in Figures 1(a) and 1(b).

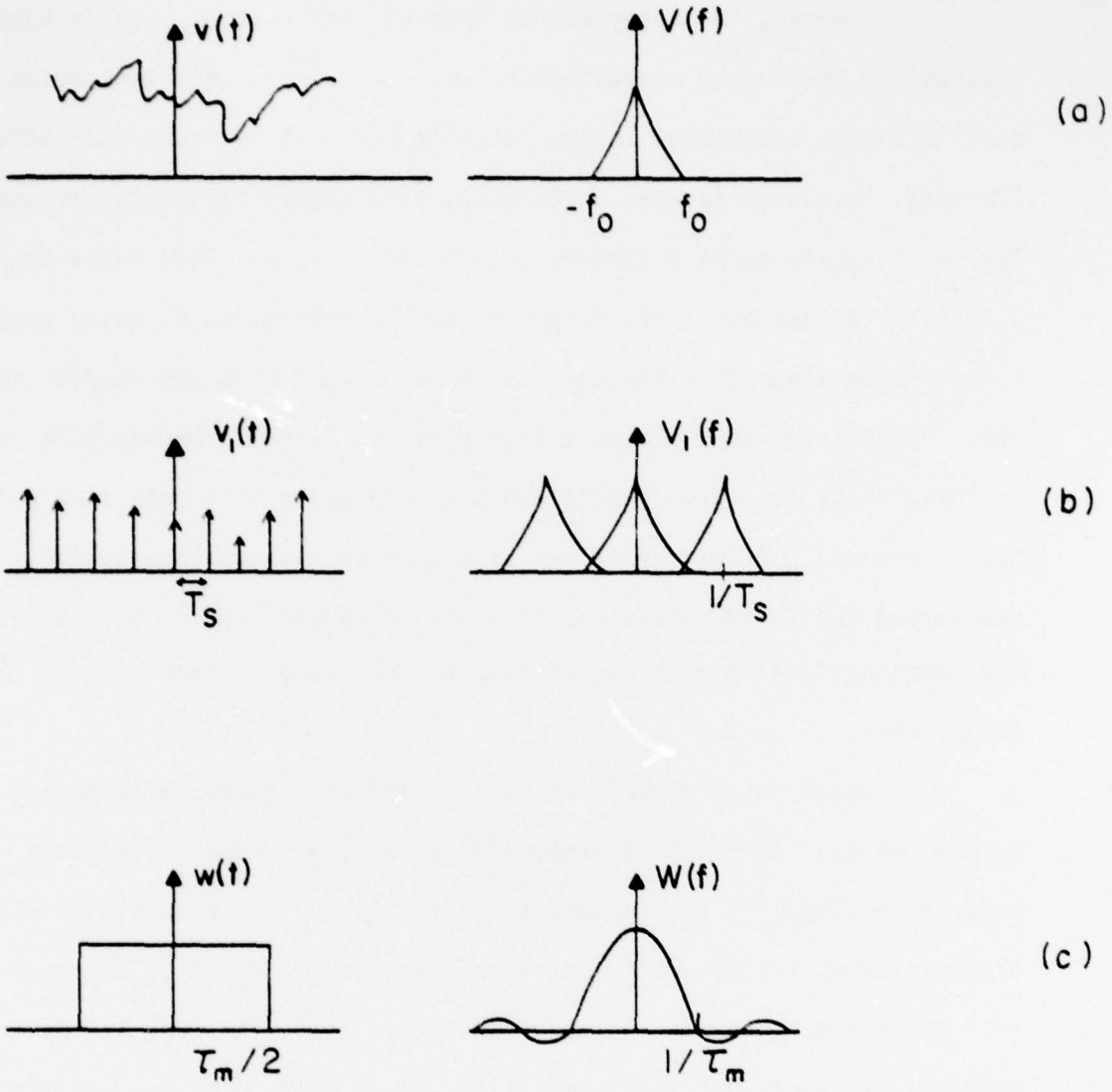

Figure 1 The time dependence and the frequency spectra of (a) a noise signal, (b) the impulse train and (c) the box function.

However, the Paley-Wiener theorem[3] states that exactly band limited filters are physically unrealizable, and our original wideband noise function must have some components in the range of $f>f_0$. This means that adjacent identical frequency spectra do overlap, so a higher frequency component at f_0+f will appear to be a spectral component at f_0-f. This false appearance is called "aliasing." This error is normally minimized by using good filters and choosing a sampling frequency somewhat larger than the theoretical minimum. We will use an additional factor of ten so that the sampling frequency is $20f_0$. This will give negligible aliasing error with only simple filters. Also, because of an additional restraint on the autocorrelation function resolution due to the numerical integration we will use to obtain the spectrum, the sampling frequency is higher than is necessary to merely limit the "aliasing" error.

The Nyquist theorem assumes an infinite number of samples, and, of course, we are limited to a finite sampling time. This corresponds mathematically to multiplying the impulse train in time by a box function of length, τ_m, or convoluting the frequency spectrum with the transform of the box, $(\sin\pi f\tau_m)/\pi f$. These functions are indicated in Figure 1(c). As long as the frequency spectrum is fairly constant over intervals of $\frac{1}{\tau_m}$ or less, the $(\sin\pi f\tau_m)/\pi f$ function can be approximated by an impulse, and the convolution does not change the spectrum. Thus, the minimum frequency resolution is $\frac{1}{\tau_m}$ because this function smears out or averages over that frequency interval.

Finally, there is error associated with the finite length of time required to obtain a point sample due to the signal fluctuation over that time. This time is associated with the particular sample-hold or analog-digital (A-D) converter device employed. We require a 200KHz maximum sampling frequency corresponding to a 10KHz maximum signal frequency and propose using an A-D

converter with a 2 μs conversion time for the four bits we will need. This provides a factor of 50 between the nominal maximum frequency and the conversion frequency. Also, the full scale fluctuation must be allocated for in a wideband noise signal, and the very highest frequency components alone would not be expected to have anything close to full scale amplitudes. We will find that the individual sampled point quantization error due to the small number of bits used will be much larger than the A-D conversion time error.

In order to calculate the frequency spectrum, S(f) of a time function, v(t), it is first desirable to calculate the autocorrelation function given by

$$\psi(\tau) = \overline{v(t)v(t+\tau)} \tag{1}$$

where τ is the delay time in integer multiples of the sampling period. Then the frequency spectrum is obtained through the Wiener-Khintchine integral,

$$S(w) = 4\int_0^\infty \psi(\tau)\cos\omega\tau d\tau \tag{2}$$

There is also an inverse integral for the autocorrelation function given by

$$\psi(\tau) = \frac{1}{2\pi}\int_0^\infty S(\omega)\cos\omega\tau d\omega \tag{3}$$

The correlator has the job of sampling at high speed, calculating the autocorrelation function, and storing it for introduction into a software integration program or a Fourier analyzer.

The numerical integration can take significant time, so the choice of procedure used is critical. In particular, an appropriate range of fre-

quency must be chosen. If single decade frequency spectra are desired, a 200 point autocorrelation function must be calculated. This is because we need a sampling rate 20 times the highest frequency, as discussed before, and a total sample time equal to the period of the lowest frequency to insure good frequency resolution. A two-decade spectrum can be obtained in one of two ways. First, two single-decade spectra can be patched together. This requires twice the integration time and, if a higher frequency decade is added, 10% more correlation time. The other alternative is a continuous two-decade spectrum. However, this requires a 2000 point autocorrelation function, increasing the required integration time and the storage capacity by a factor of 10. It does eliminate the 10% increase in correlation time, since the additional points are obtained by increasing the sample rate rather than the total time, but this does not offset the other problems. Anything less than one decade, however, obviously does not experience this order of magnitude gain in time and memory, so one decade seems to be the choice.

In any calculation based on experimental results, there is error associated with the finite limits of the Wiener-Khintchine integrals. For example, if we have a noise spectrum that is flat between ω_1 and ω_2, i.e. $S(\omega)=1$, and zero elsewhere, the autocorrelation function from Equation (3) is

$$\varphi(\tau) = \frac{1}{2\pi}\int_{\omega_1}^{\omega_2} S(\omega)\cos\omega\tau d\omega$$
$$= \frac{1}{2\pi\tau}(\sin\omega_2\tau - \sin\omega_1\tau) \qquad (4)$$

The calculated power spectrum, $S'(\omega)$ is then

$$S'(\omega) = 4\int_0^{\tau_m} \frac{1}{2\pi\tau}(\sin\omega_2\tau - \sin\omega_1\tau)\cos\omega\tau d\tau$$

$$= \frac{1}{\pi}[\mathrm{Si}(\omega_2+\omega)\tau_m + \mathrm{Si}(\omega_2-\omega)\tau_m - \mathrm{Si}(\omega_1+\omega)\tau_m$$

$$- \mathrm{Si}(\omega_1-\omega)\tau_m] \qquad (5)$$

where

$$\mathrm{Si}(x) = \int_0^x \frac{\sin t}{t}\, dt \qquad (6)$$

In a typical case, $\frac{\omega_1}{2\pi}$ is one-half the lowest frequency in the one-decade spectrum of interest and $\frac{\omega_2}{2\pi}$ is twice the highest frequency. This is an approximation, since the filter rolloff is sharp but finite. If we assume, from our previous analyses, that $\tau_m = \frac{1}{2(\omega_1/2\pi)}$, then we have

$$\omega_1\tau_m = \pi$$

$$\omega_2\tau_m = 40\pi$$

$$\omega\tau_m = 2\pi \rightarrow 20\pi \qquad (7)$$

The function Si(x) can be closely approximated by

$$\mathrm{Si}(x) \approx \frac{\pi}{2} - f(x)\cos(x) - g(x)\sin(x) \qquad (8)$$

where, for $x \geq \pi$, we have

$$f(x) \approx \frac{1}{x}$$

$$g(x) \approx \frac{1}{x^2} << f(x) \qquad (9)$$

Because $\omega_2\tau_m$ is so large, the first two terms in the expression for $S'(\omega)$ can be approximated by $\frac{\pi}{2}$, so that we get

$$S'(\omega) \approx \frac{1}{\pi}\left[\frac{\pi}{2} + \frac{\pi}{2} - \frac{\pi}{2} + \frac{\cos(\omega+\omega_1)\tau_m}{(\omega+\omega_1)\tau_m} + \frac{\pi}{2} - \frac{\cos(\omega-\omega_1)\tau_m}{(\omega-\omega_1)\tau_m}\right]$$

$$= 1 + \frac{1}{\pi}\left[\frac{\cos(\omega+\omega_1)\tau_m}{(\omega+\omega_1)\tau_m} - \frac{\cos(\omega-\omega_1)\tau_m}{(\omega-\omega_1)\tau_m}\right] \qquad (10)$$

where we used $Si(x) = -Si(-x)$ in the last term. Obviously the assumed spectrum is recovered in the first term, but there is an error given by the second and third terms.

A similar calculation for $S(\omega) = \frac{1}{\omega}$ gives

$$S'(\omega) \approx \frac{1}{\omega}\{1 - \frac{1}{\pi}[2\sin(\omega\tau_m)Ci(\omega_1\tau_m) + \frac{\cos(\omega+\omega_1)\tau_m}{(\omega+\omega_1)\tau_m}$$

$$+ \frac{\cos(\omega-\omega_1)\tau_m}{(\omega-\omega_1)\tau_m}]\} \qquad (11)$$

where

$$Ci(x) = \int^{\infty} \frac{\cos(t)}{t}\, dt \qquad (12)$$

We can make $Ci(\omega_1\tau_m)$ zero by appropriate choice of ω_1 (e.g. $\omega_1\tau_m = 3.4$), giving an error result very similar to Equation (10),

$$S'(\omega) = \frac{1}{\omega}\left[1 - \frac{1}{\pi}\frac{\cos(\omega+\omega_1)\tau_m}{(\omega+\omega_1)\tau_m} + \frac{\cos(\omega-\omega_1)\tau_m}{(\omega-\omega_1)\tau_m}\right] \qquad (13)$$

The actual error is dependent on ω_1 and also on the exact form of the filtering at ω_1 which has been idealized in the above calculation. However, for $\omega_1\tau_m=3.4$, which corresponds to a minimum cutoff frequency of 0.41 times the lowest frequency in the calculated spectrum, the error is about 3% maximum for the assumed flat spectrum and about 7% maximum for the assumed 1/f spectrum. This value of f_1 is reasonable from the standpoint of eliminating unwanted frequencies without altering the desired spectral components.

The theoretical calculation is useful for obtaining the gross features of this error, but, because of the ideal spectra that were assumed, it is doubtful that the calculation can be used to subtract out the error. The best way to eliminate it is to simply average over $\Delta\omega=\frac{2\pi}{\tau_m}$ and smooth the calculated spectrum. This point illustrates the true nature of this error. It is the frequency resolution error in the Wiener-Khintchine integral predicted by the Nyquist theorem due to the finite sampling time, τ_m. If $\tau_m \to \infty$, the error is zero for all spectra. It is true that the error is also zero for $\omega_1=0$ in the flat spectrum [Equation (10)], but the concept of frequency resolution is irrelevant if there is no structure in the spectrum.

III. NOISE SAMPLE TIME

The magnitude of a particular frequency component in a noise signal will vary statistically in time. Therefore, it is important to know how long the signal must be sampled in order to obtain a good average. Van der Ziel[4] has derived this result for an RC filter of time constant, T, and found the relative accuracy to be $1/\sqrt{2BT}$ for a bandwidth, B, in the signal. We will follow his derivation but modify it to our sampling technique.

Let $x(t)$ be the random input to a quadratic detector with a current output of $I=x^2$. We want to average long enough to get $\overline{I}$. The autocorrelation of the error is $\overline{[I(t)-\overline{I}][I(t+\tau)-\overline{I}]}$. Van der Ziel[4] shows that

$$\overline{[I(t)-\overline{I}][I(t+\tau)-\overline{I}]} = 2\overline{I}^2c^2(\tau) \tag{14}$$

where $c(\tau)$ is the normalized autocorrelation function of $x(t)$ given by

$$c(\tau) = \overline{x(t)x(t+\tau)}/\overline{x}^2 \tag{15}$$

The spectral intensity of the error is given by the Wiener-Khintchine integral of equation (2), namely

$$\begin{aligned} S(\omega) &= 4\int_0^\infty \overline{[I(t)-\overline{I}][I(t+\tau)-\overline{I}]}\cos\omega\tau d\tau \\ &= 4\int_0^\infty 2\overline{I}^2c^2(\tau)\cos\omega\tau d\tau \end{aligned} \tag{16}$$

The autocorrelation function of a square band of intensity, S_0, bandwidth, B, and center frequency, f_0, is given by the inverse Wiener-Khintchine integral:

$$\begin{aligned} c'(\tau) &= \frac{1}{2\pi}\int_0^\infty S'(\omega)\cos\omega\tau d\omega \\ &= S_0\int_{f_0-B/2}^{f_0+B/2}\cos 2\pi f df \\ &= S_0(\sin\pi B\tau)(\cos 2\pi f_0\tau)/\pi B\tau \end{aligned} \tag{17}$$

We know that $\overline{I} = \overline{x^2} = S_0B$, so, from Equation (15),

$$c(\tau) = c'(\tau)/S_0B$$

$$= (\sin\pi B\tau)(\cos 2\pi f_0\tau)/\pi B\tau \qquad (18)$$

Inserting this $c(\tau)$ into Equation (16) gives

$$S(f) = 2S_0^2(B-f) \qquad 0<f<B$$

$$= 0 \qquad f>B \qquad (19)$$

Rather than an RC filter with a response function $(1+\omega^2\tau^2)^{-1}$, we have a sampling interval, T, that is a box, with a response function $(\sin\pi fT)/\pi fT$. Thus, integrating over frequency to get the fluctuating output, $\bar{Y}^2$, we have

$$\bar{Y}^2 = \int_0^B 2S_0^2(B-f)\,\frac{\sin\pi fT}{\pi fT}\,dt$$

$$= 2S_0^2\int_0^{B\pi f}\left[\frac{B}{\pi T}\,\frac{\sin(x)}{x} - \frac{\sin(x)}{\pi^2T^2}\right]dx \qquad (20)$$

where $x = \pi fT$.

If we let T get very large relative to B, the second term goes to zero and the integral of $\frac{\sin(x)}{x}$ goes to $\frac{\pi}{2}$, so that

$$\bar{Y}^2 = S_0^2B/T \qquad (21)$$

and the relative error is

$$\sqrt{\overline{Y^2}/\overline{I^2}} = (BT)^{-1/2} \qquad (22)$$

There is a small difference of $\sqrt{2}$ from the RC time constant result.

From chapter two, we know that B is simply the reciprocal of the maximum autocorrelation delay, $1/\tau_m$. As we shall see in the next chapter, we will average n autocorrelation functions to get the final result, so the measuring time is $T = n\tau_m$. This gives a relative error of $(\frac{1}{\tau_m} \times n\tau_m)^{-1/2} = (n)^{-1/2}$, and n is chosen to get the desired accuracy (e.g. 5% requires n=400).

IV. CORRELATION PROCEDURE

Normally, the autocorrelation function is obtained by sampling 2n points at equal intervals. Each of the first n points is then multiplied by the next n points to get n x n products. The n products with the same delay between the two sampled points are then added together and divided by n to get an average. This provides one point in an n-point autocorrelation function based on Equation (1).

A software program was written to perform this calculation and an example of the result is shown in Figure 2 for a 0.2Hz sine wave and two different amplitudes. The autocorrelation function of Figure 2a and the Wiener-Khintchine integral or power spectrum in Figure 2b are both software calculations performed on a Wang 720C desk calculator. The autocorrelation function requires about eight minutes and power spectrum about thirty minutes when a 200 point autocorrelation function is used to calculate a 40 point power spectrum. Most of the 40 points in this case are off the scale. The Wang machine was used because the sampling hardware was readily available and

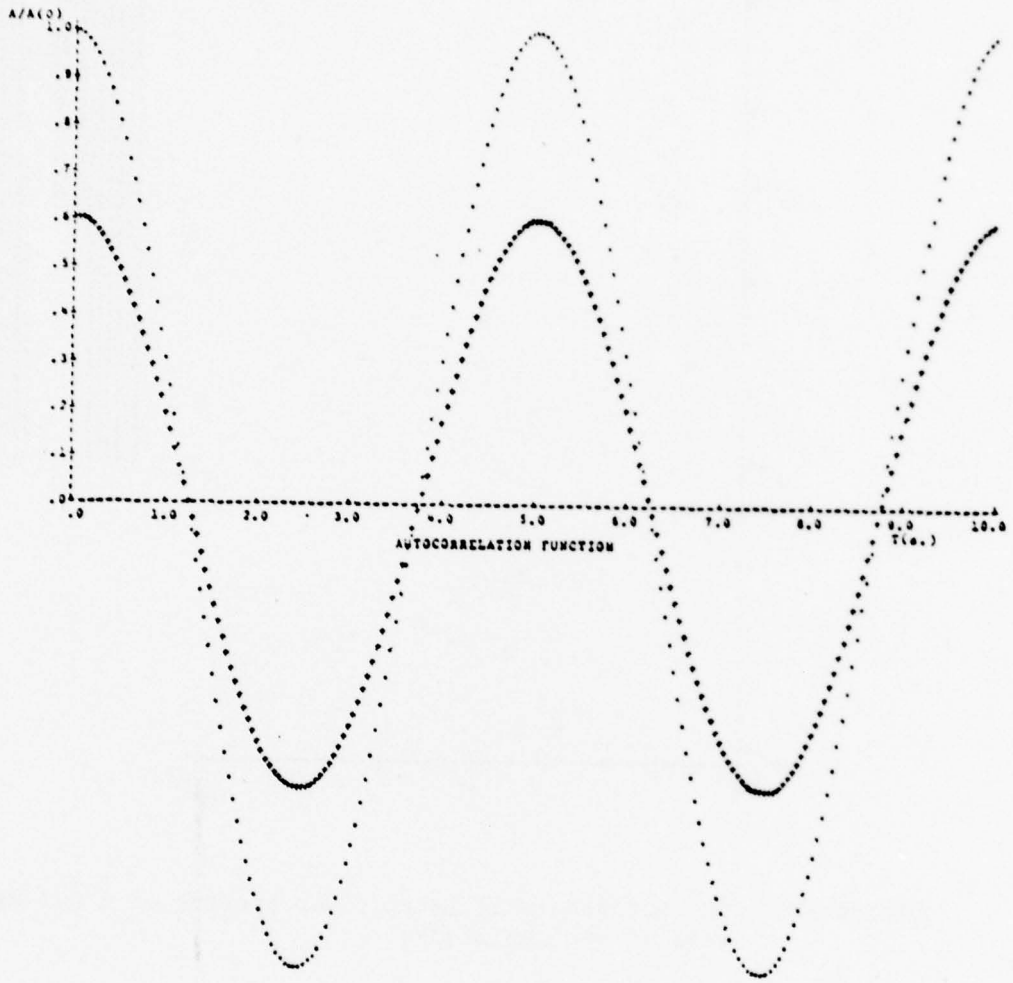

Figure 2(a) The software calculated autocorrelation function of a 0.2 Hz sine wave at two amplitudes.

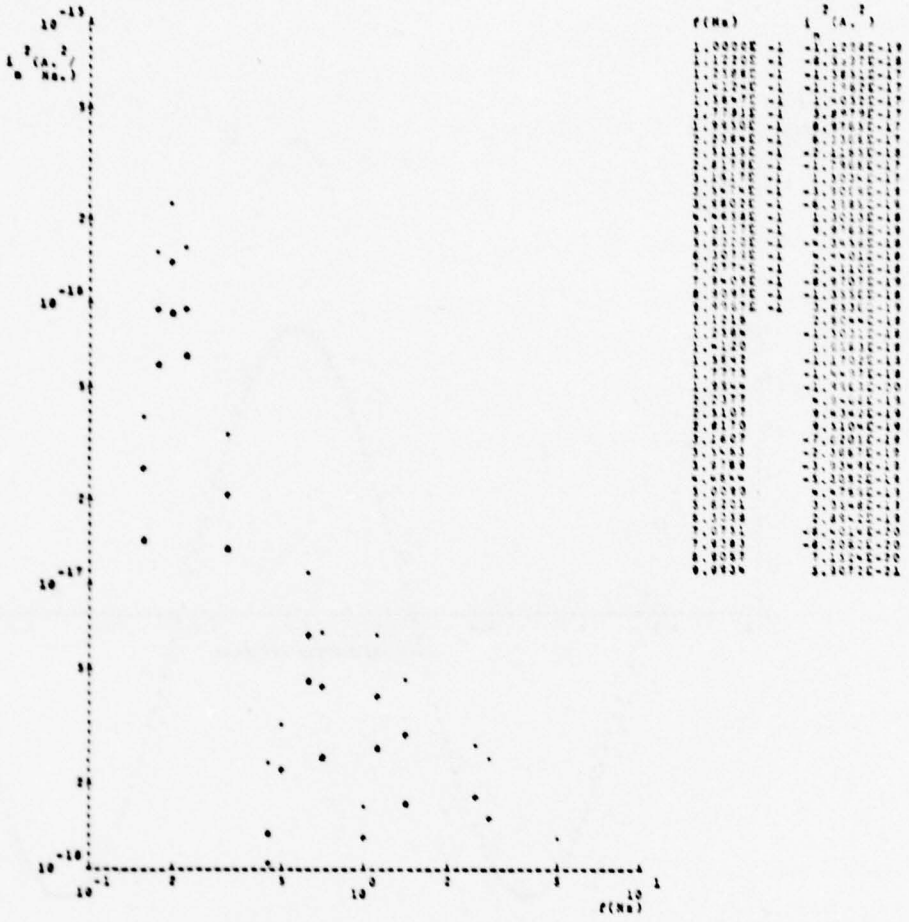

Figure 2(b) The software calculated power spectra of a 0.2 Hz sine wave at two amplitudes.

this machine is inexpensive enough to dedicate to a simple task. However, the machine is limited in its sampling and computation speed. Faster machines could be employed to speed up the computation, but the slow sampling rate of about 100Hz is general to all but very expensive and sophisticated equipment.

At the very least, then, some sort of high-speed buffer is necessary to sample and store the data prior to transmission to the computer. Given this prospect, it is reasonable to include hardwired computation in the sampling buffer, particularly when noise correlation is proposed. In the example of Figure 2. we had a signal which is nonstatistical, thus, only one autocorrelation function is required. However, from chapters two and three, we know that 400 autocorrelation functions, each requiring 400 sampled points, are necessary to get a good time-averaged one-decade noise spectrum. If all the points are sampled and stored, this requires 160,000 words of memory. If the calculations are made after each 400 point block is sampled, then only a 200 word cumulative memory for the averaged autocorrelation function plus a 400 word memory for one sampled block is required. However, eight minutes of computation would transpire between samples, greatly increasing the total sampling time and causing problems of drift control. A faster machine could reduce the computation time to a few seconds, but the sampling time alone can be several hours and this would entail too much use of an expensive machine.

In order to avoid these problems, the concept of incomplete correlation can be effectively used. This term describes a scheme in which the first sampled point is multiplied by the next n points to get a crude autocorrelation function. Because all the points are not correlated with each other, incomplete use is made of the available data and more samples must be taken. Only one of the n points is correlated, so we use $\frac{1}{n}$ of the available information. In our one decade frequency spectrum with a 200 point autocorrelation function we expect to use 1/200 of the possible data.

Actually, the information loss is not that severe. For perfectly band-limited spectra, the Nyquist criterion requires a 20 point autocorrelation function for a one decade spectrum. We increased that to 200 to account for imperfect band limiting and to increase the resolution of the autocorrelation function, but the order of magnitude increase in data gives nothing like a factor of 10 increase in information. Therefore, the information loss factor due to incomplete correlation is between 20 and 200, probably closer to 20. This is also the increased time factor required for a fixed accuracy in a modified Equation (22).

In order to verify this analysis, autocorrelation functions were calculated over various numbers of sample sets using a software simulation of incomplete correlation. For each number of sample sets or total time interval, eight functions were computed and a percent variance at particular frequencies in the computed spectra were calculated. The input was white noise limited to 1.0Hz and sampled at 20Hz. The dots in Figure 3 represent these experimental results at two frequencies, while the solid lines are the theoretical predictions from Equation (22). Note that this data lies generally between the 20 and 200 information loss factor corrections and follows the slope of these lines.

Offsetting the increased time required for sampling by the use of incomplete correlation is the complete elimination of computation time. This is accomplished by hardwiring an asynchronous calculator of the autocorrelation function that takes place between sample times up to a rate of 100KHz. This is impossible to do for complete correlation because of the lengthy clocked calculations required unless all 200 points are calculated in parallel. Hardwiring this parallel calculation is impossible for cost and size reasons.

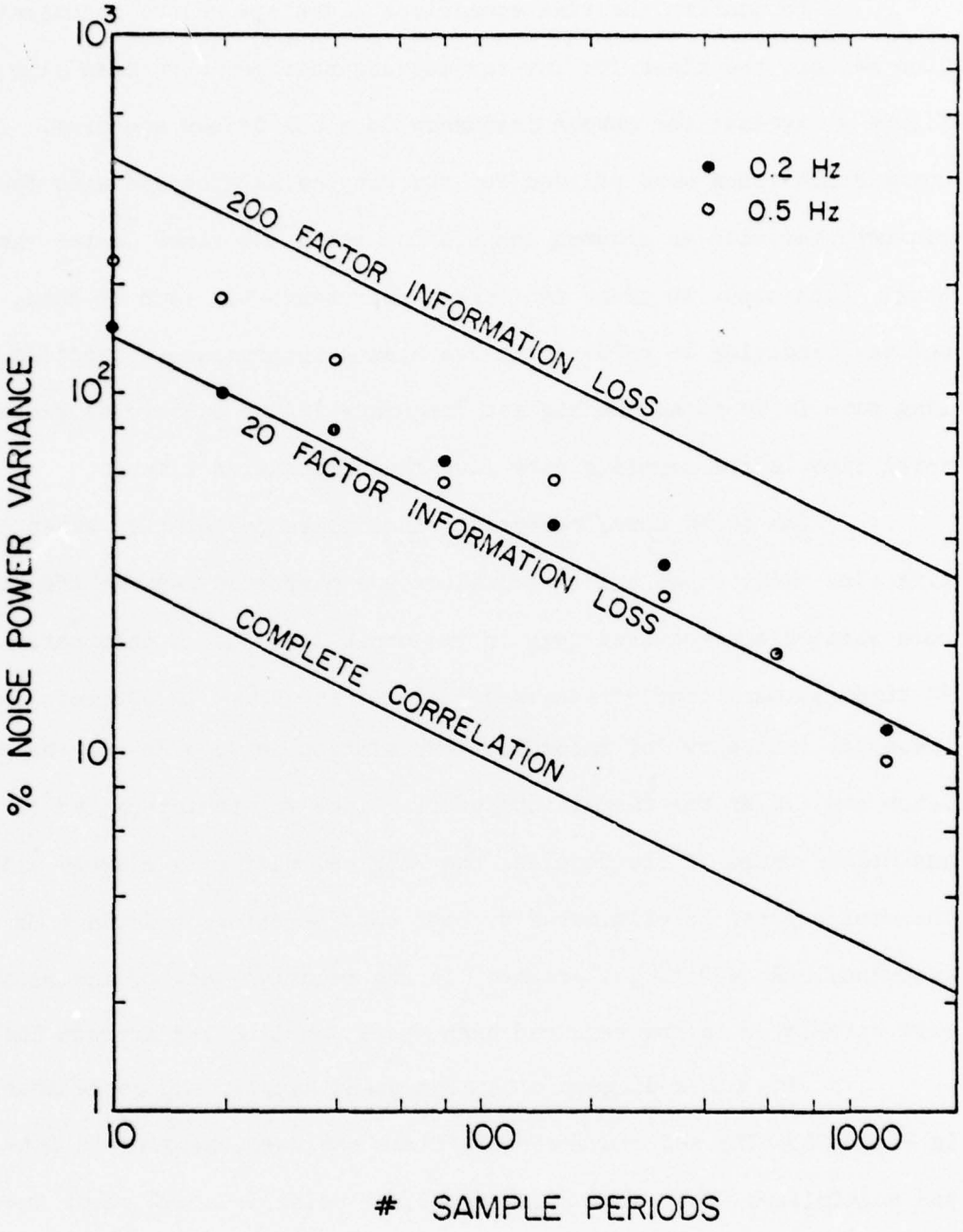

Figure 3 The percentage noise power variance as a function of the number of sample periods with incomplete correlation as a parameter.

To confirm the time comparison advantage of the incomplete correlation method, the times for the various alternatives have been plotted in Figure 4 against the lowest frequency in a one decade spectrum. The complete correlation times were plotted for the Wang calculator and also for a HP21MX minicomputer with an assumed computation speed 100 times faster than the Wang. Each point on these two curves represents 400 sets of data, each of 400 points, resulting in a 200 point averaged autocorrelation function. The sampling rate is 20 times the highest frequency in the one decade range, and the total time is the sampling time plus the computation time.

The third curve represents incomplete correlation based on the sampling time only, since all calculations are performed between the samples. More samples are required than in the other case due to information loss, so 30 times as many samples are used to get this curve, 12,000 sets in all. The crossover frequency for incomplete correlation is 0.06 Hz for the Wang calculator and 6.0 Hz for the minicomputer. Since we are interested in a 0.1 Hz and higher range of frequencies, the Wang calculator is clearly eliminated. The minicomputer is eliminated by cost considerations and the 6 Hz corssover frequency. An additional argument is the relative ease of including a hardware correlator in the required high speed sampling and storage buffer.

The block diagram of a high speed sampler and correlator is shown in Figure 5. The A-D converter digitizes the data, passing it into the latch and multiplier. The latch holds the first point in a 200 point set, so that it is multiplied by every other point as well as itself. These products are fed into the adder, where they are added to the cumulative total in the shift register memory. The shift register memory is 200 bits long, so that the delay between the two multiplied points remains synchronized with the shift register memory. There are several shift registers, latches, adders, etc., in parallel

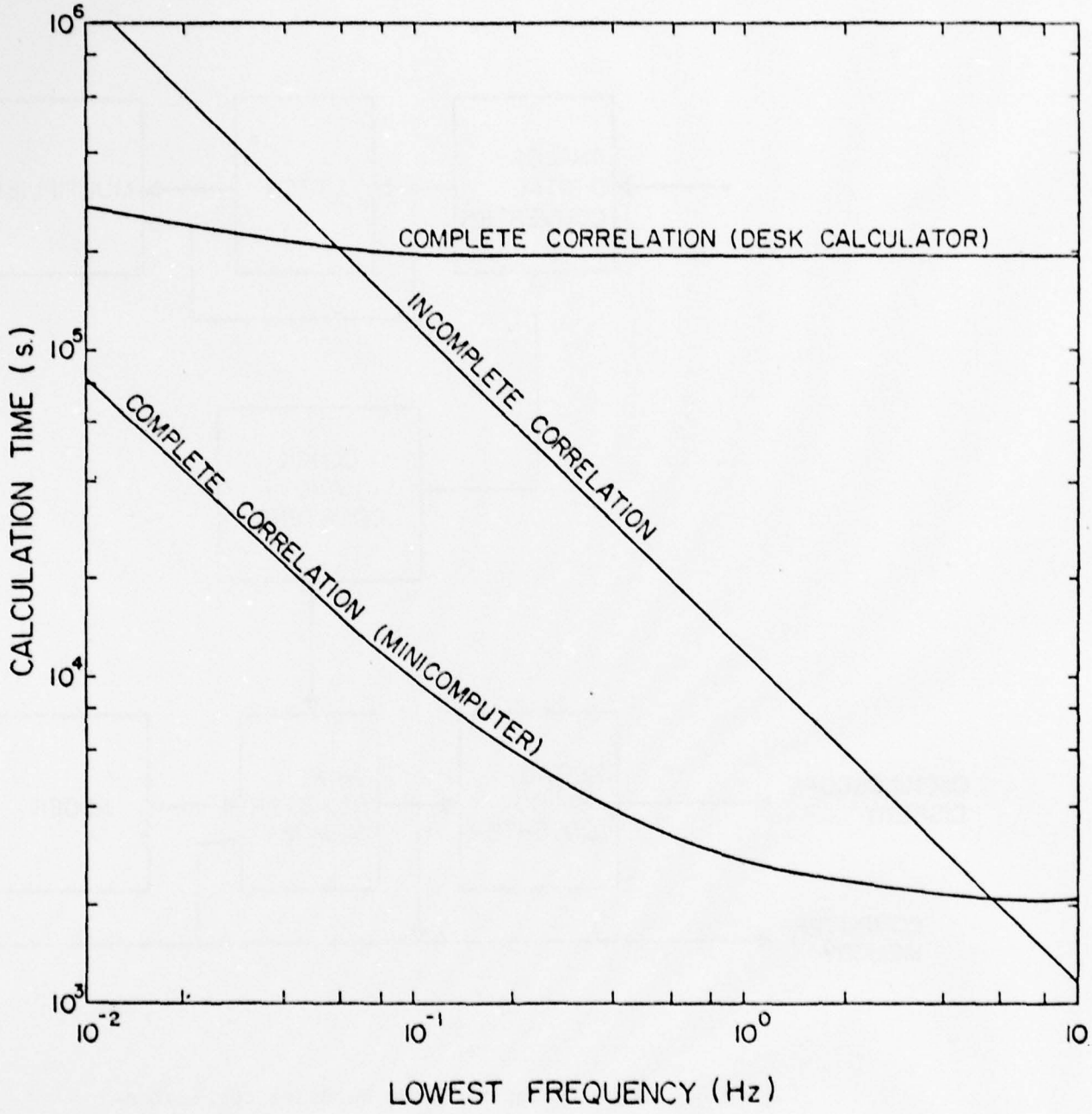

Figure 4 The calculation times as a function of the lowest frequency for complete and incomplete correlation using a desk calculator or a minicomputer.

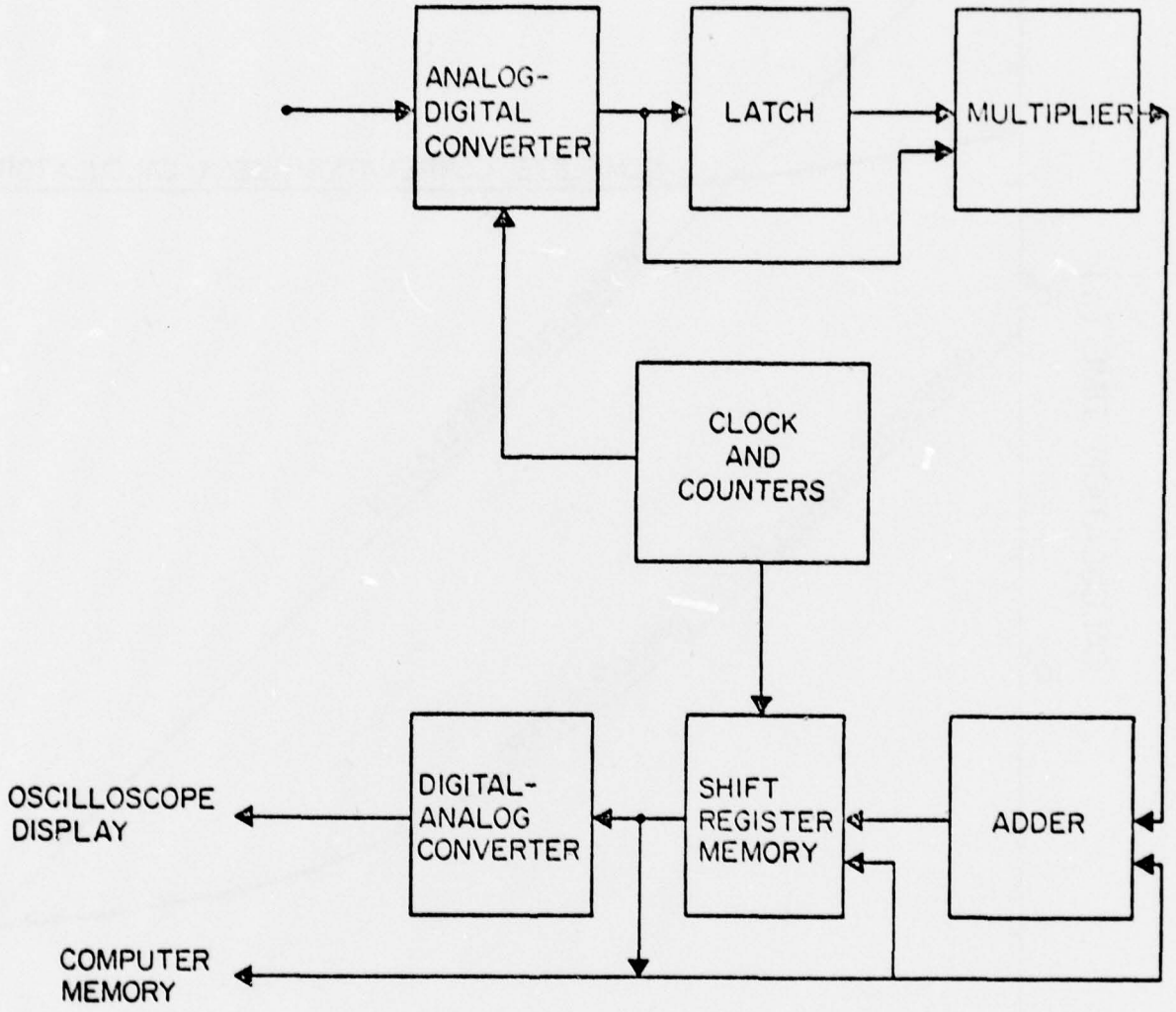

Figure 5 The box diagram of the hardware correlator.

to process multibit numbers. A clock pulses the A-D coverter, the latch, the shift registers, and the controlling counters. One counter counts the 200 points in a data set, and the other counter counts the number of data sets. A digital-analog converter is used to reconvert the data stored in the shift register for oscilloscope display. The shift register data is also available for output to a computer for computing the power spectrum from the autocorrelation function at a later time. Note that the multiplication and addition is completely asynchronous and requires only about 100 nanoseconds. This means that the A-D converter is the limiting factor in determining sampling speed. At the present time (January 1976), eight bit converters with 2 μs conversion times are available for about $100. Thus, we can easily contemplate 200 KHz clock rates.

V. QUANTIZATION AND SAMPLING ERROR

The number of digital bits required for good accuracy should be known because it can drastically affect the hardware cost and speed performance. The speed/cost ratio of the A-D converter is inversely proportional to the number of bits required. Also, the multipliers and adders are generally four bit chips. The adders can be wired in parallel, but eight bit multipliers are generally more complicated than simply two four-bit multipliers. Additional logic and shift registers are also required to accommodate more bits.

Although superficial analysis indicates that the full scale accuracy of an n-bit calculation is no better than $100/2^n$%, the fact that we are analyzing a randomly distributed noise signal allows us to do much better. Widrow[5] has used distribution functions and their transforms to indicate that this is indeed so. A graphical depiction of this analysis which is similar to Figure 1 for the Nyquist criterion is shown in Figure 6. The Gaussian distribution

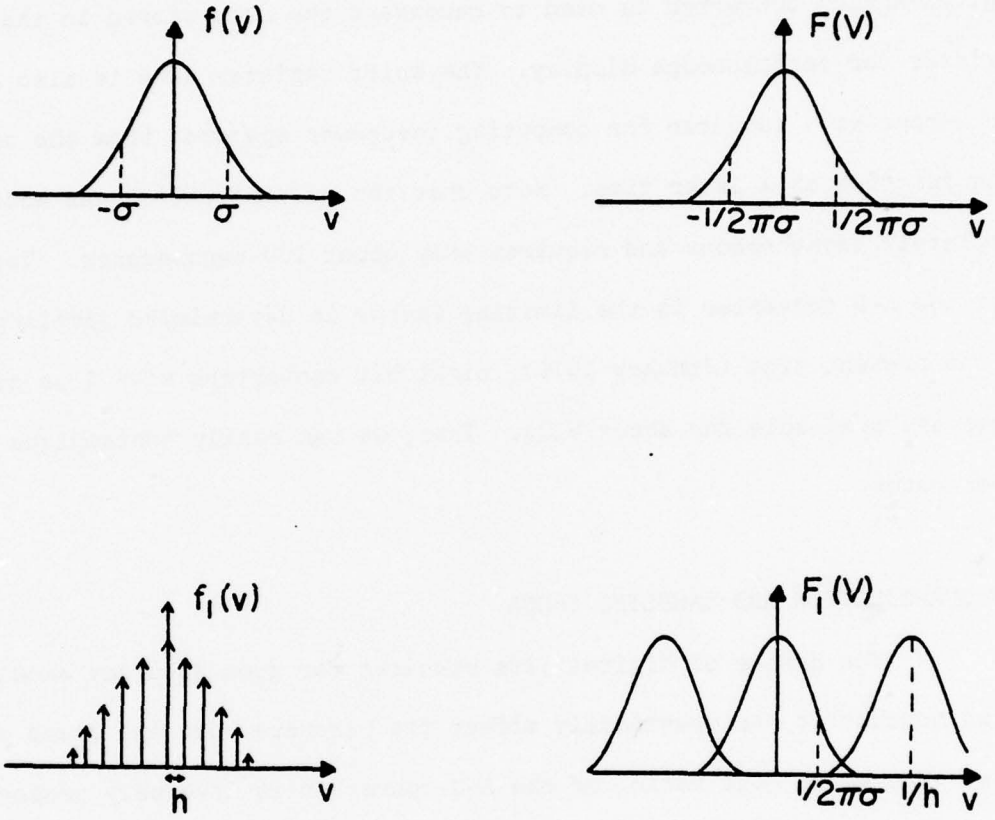

Figure 6 The noise voltage amplitude distribution function and its Fourier transform.

of the noise vs voltage is denoted by $f(v)$, where σ is the root mean square or standard deviation. However, $f_1(v)$ is the experimental distribution obtained from the quantized data, since only data separated by the bit size, h, is available. $F(V)$ is the transform of $f(v)$, and $F_1(V)$ is the transform of $f_1(v)$. Note that $F(V)$ is recoverable from $F_1(V)$ as long as $\frac{1}{2h} >> \frac{1}{2\pi\sigma}$ or $h << \pi\sigma$.

A good 1% accuracy criterion would require having the overlap at least three standard deviations down the Gaussian curve so that $\frac{1}{2h} \geq \frac{3}{2\pi\sigma}$ or $\sigma > \frac{6h}{2\pi} \approx h$. We should also insist on having at least four standard deviations on either side of the distribution center within the full scale limits. This will prevent clipping of the signal. A four bit machine has sixteen possible numbers, dividing the full scale into eight units of width h on each side of zero. Thus, we can have $\sigma = 2h$, which would give total accuracy significantly greater than 1%.

Widrow's use of Fourier transforms is very enlightening, but a simple integration of the distribution function over the quantization error can give a good series solution that converges rapidly for $\sigma \leq h$ and also indicates how the total error varies with σ and the true average. To do this, we define a function, ROUNDv, which rounds off any v to the nearest available bit. This results in a staircase function with each step of width h. The normalized functions, v/h, $(v/h)^2$, ROUND v/h and $(\text{ROUND } v/h)^2$ are plotted against v/h in Figure 7. The function ROUND v/h is zero for $-\frac{h}{2} < v < \frac{h}{2}$ and has values which are integral multiples of h. The error at each v is the difference between this function and the $f(v)=v$ function. If we integrate this error over the distribution function, the error resulting in the average of many samples is calculated.

Thus, we have

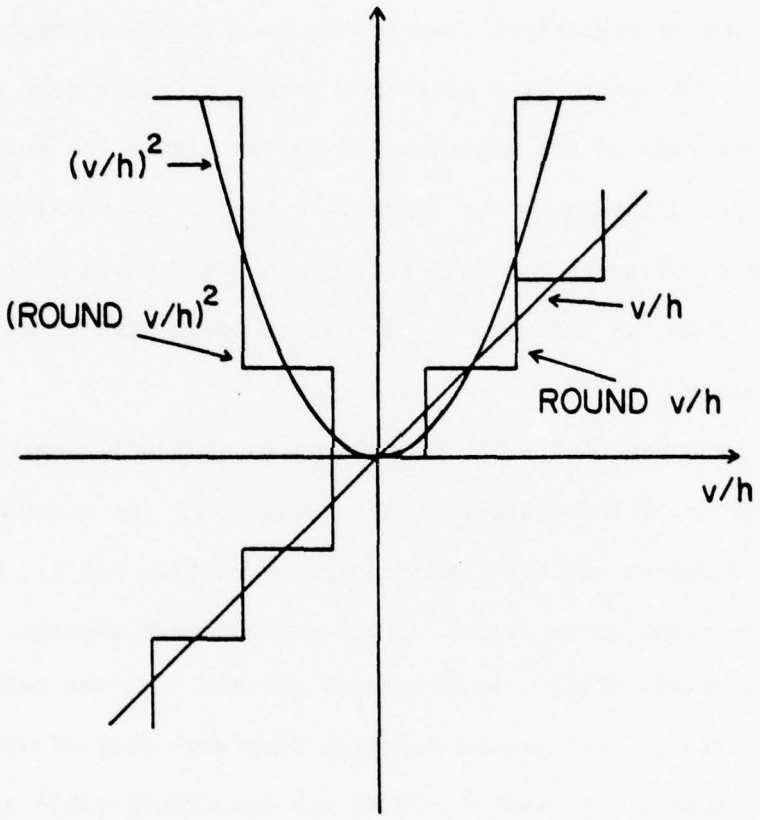

Figure 7 The round-off function, ROUNDv, as a function of the normalized voltage v/h.

$$E = \frac{1}{\sqrt{2\pi}\sigma} \int_{-\infty}^{\infty} (\text{ROUND}v - v)\exp[-(v-V)^2/2\sigma^2]\, dv \qquad (23)$$

where E is the error and V is the true average of the distribution. The second term is simply the average of v or V, giving

$$E = \frac{1}{\sqrt{2\pi}\sigma} \int_{-\infty}^{\infty} (\text{ROUND}v)\exp[-(v-V)^2/2\sigma^2]dv - V \qquad (24)$$

Because ROUNDv is discontinuous, the integral must be integraged piecewise, or

$$E = \frac{1}{\sqrt{2\pi}\sigma} \sum_{n=-\infty}^{\infty} \int_{h(n-\frac{1}{2})}^{h(n+\frac{1}{2})} nh\, \exp[-(v-V)^2/2\sigma^2]dv - V \qquad (25)$$

Changing variables, we let $x = (v-V)\sqrt{2}\sigma$ so that

$$E = \frac{1}{\sqrt{\pi}} \sum_{n=-\infty}^{\infty} \int_{[n-\frac{1}{2}-V/h]h/\sqrt{2}\sigma}^{[n+\frac{1}{2}-V/h]h/\sqrt{2}\sigma} nh\, \exp(-x^2)dx - V \qquad (26)$$

Finally, we use

$$\int_0^{\infty} e^{-x^2} dx = \frac{\sqrt{\pi}}{2} \text{erf}(x) \qquad (27)$$

so that

$$E = \frac{h}{2} \sum_{n=-\infty}^{\infty} n\{\text{erf}[(n+\tfrac{1}{2} - V/h)h/\sqrt{2}\sigma] - \text{erf}[(n-\tfrac{1}{2} - V/h)h/\sqrt{2}\sigma]\} - V \qquad (28)$$

A graph of this error is plotted in Figure 8 against the average voltage, V. Both axes are normalized to h, as is the parameter, σ. For $\sigma = 0.5h$, the error is already down to $0.0023h$, which is very small. The $\sigma=0$ curve represents the other extreme, where the total error is identical to the error of a single sampled point. Mathematically in this case, the distribution function is an impulse centered at V, so the integral simply gives the single point error at V.

In our situation, we are interested in noise power, so we would like to get the error in v^2. To do this, we again integrate the distribution function over the error, in this case $(\text{ROUND}v)^2 - v^2$. Just as in Equation (28), the second term in the integrand gives the true average which is now $\overline{v^2} = \sigma^2 + V^2$, and the total result is

$$E = \frac{h^2}{2} \sum_{n=-\infty}^{\infty} n^2 \{\text{erf}[(n+\tfrac{1}{2} - V/h)h/\sqrt{2}\sigma] - \text{erf}[(n-\tfrac{1}{2} - V/h)h/\sqrt{2}\sigma] \} - (\sigma^2 + V^2) \tag{29}$$

A graph of this error is given in Figure 9 plotted against the normalized voltage, V/h, with σ as a parameter. Note that the error saturates for large σ at $.083h^2$ or $h^2/12$.

The factor $h^2/12$ can be understood by treating the quantization error as an additional noise source. Katzenelson[6] has shown that the input noise signal and the quantization noise are uncorrelated, so that their autocorrelation functions can be added. Also, if σ is large, the quantization noise distribution function is not a gaussian, but a box of width h and height $\frac{1}{h}$. When the square of the quantization noise voltage, v_Q^2, is multiplied by the distri-

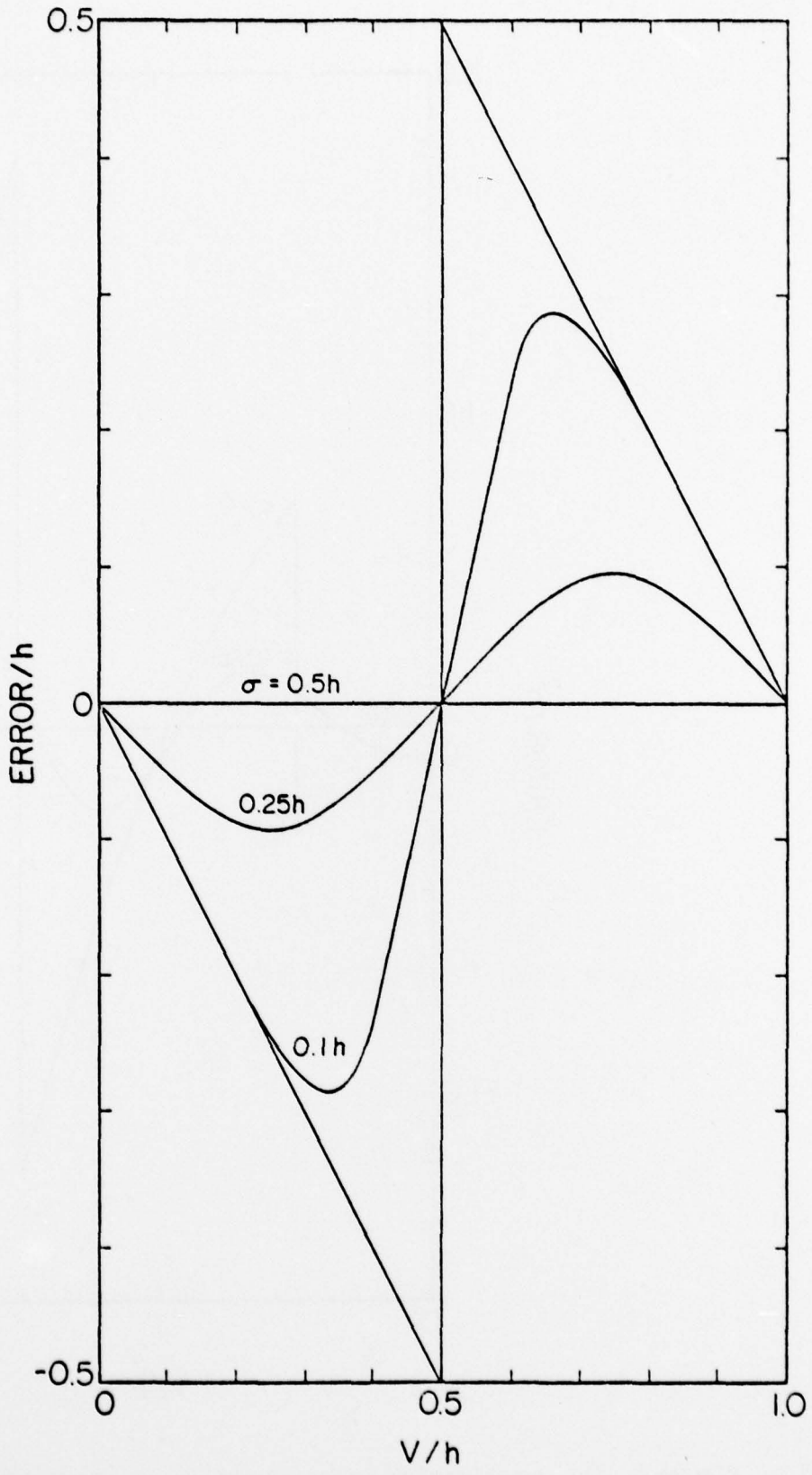

Figure 8 The quantization error of the noise voltage, v, as a function of the average voltage.

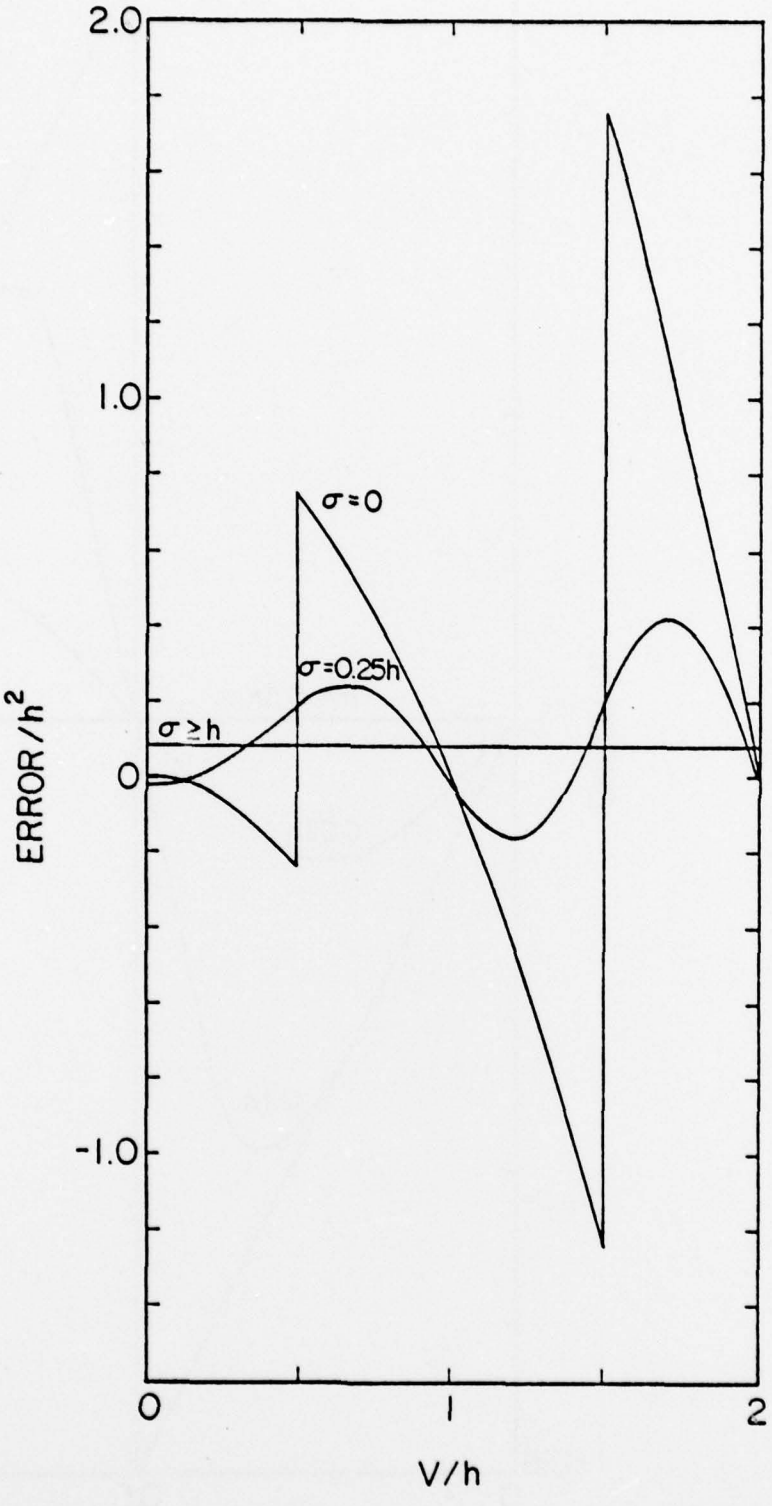

Figure 9 The quantization error of the noise power, v^2, as a function of the average voltage.

bution function and integrated, we get the autocorrelation function of the quantization noise at $\tau=0$.

$$\psi_Q(0) = \int_{-h/2}^{h/2} \frac{1}{h} V_Q^2 \, dV_Q$$

$$= h^2/12 \qquad (30)$$

Finally, we must determine how the quantization noise is autocorrelated for $\tau>0$. Widrow[5] and Katzenelson[6] have used the (1,1) moment of the transform of the distribution function to obtain

$$\rho_Q(\tau) = \frac{h^2}{12} \exp\{-4\pi^2[1-\rho(\tau)]\sigma^2/h^2\} \qquad (31)$$

where ρ_Q and ρ are the correlation coefficients of the quantization noise and the input noise signal respectively. This formula is accurate for $\rho(\tau)$ close to unity. When $\rho=1$, $\rho_Q = \frac{h^2}{12}$ as we saw before. However, if $\sigma<h$ in the exponent, ρ_Q can be expected to decrease much faster than ρ. This fact is illustrated in Figure 10. Since the second point in the autocorrelation function of the input signal would normally have $\rho<0.99$ and because we have $\sigma=2h$ in our four bit machine, the maximum error is about $0.2(h^2/12)$ for the second point and probably less than $0.05(h^2/12)$ for the others.

Actually, even the $h^2/12$ error for the $\tau=0$ point is a factor of 3 below the single point error and can be ignored for 2% accuracy. It is so easily corrected, though, that it is worthwhile to do so. For extreme cases, the $\tau>0$ error can be corrected using Equation (20) in an iterative manner. Also, these errors are small only for V near zero, such as the range of Figure

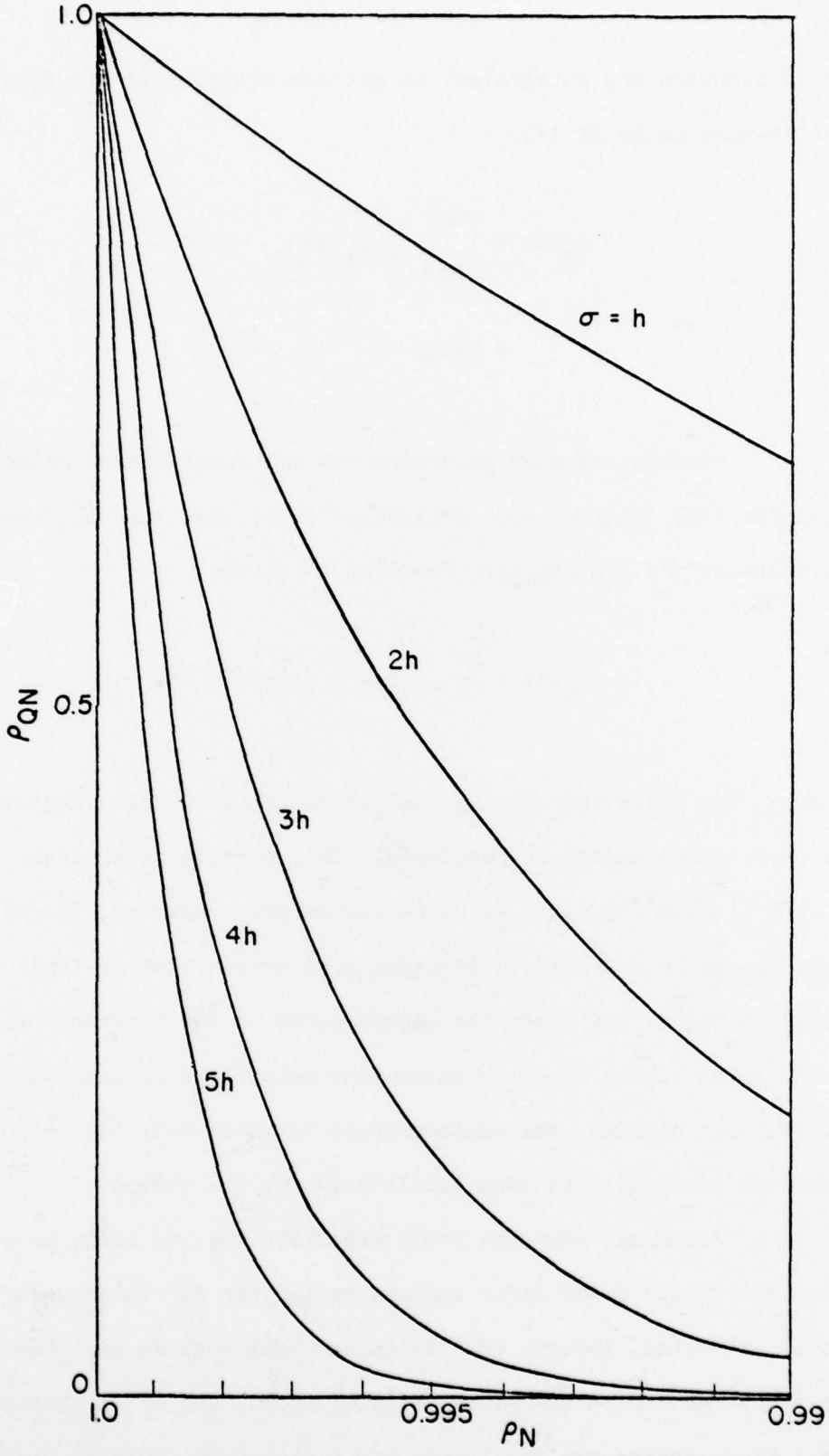

Figure 10 The correlation coefficient of the quantization noise, ρ_{QN}, as a function of the correlation coefficient of the input noise voltage, ρ_N.

9, which is normal for noise measurements. However, strongly biased signals (V>>0) could have a much larger error as indicated by the trend of Figure 9.

The preceding analysis of this chapter assumes an infinite number of points sampled so as to obtain perfect Gaussian or rectangular distribution functions. In reality, however, a finite number of sampled points yields an imperfect distribution. How much this non-ideal distribution contributes to error is the question we must address now.

It is well known[7] that if a random variable, v, is distributed with mean, V, and variance, σ^2, and a random sample of size n is taken, then the sample mean, $\bar{v}$, will be distributed with mean, V, and variance $\sigma_E^2 = \sigma^2/n$. The $\tau=0$ value of the autocorrelation function is $\sigma^2 + V^2$, so this is the reference or mean. If we want 99% assurance of accuracy, then the integral over the tail remainder in the variance distribution must be .01 or less. This occurs at $2.6\sigma_E$. A normalized error, x, then requires

$$(2.6\sigma_E)^2 = x(\sigma^2 + V^2) \tag{32}$$

We only tighten the restriction by letting V=0, so

$$(2.6\sigma_E)^2 \leq x\sigma^2$$

$$x \leq 2.6^2/n$$

$$\leq 6.76/n \tag{33}$$

Since 12,000 samples of the autocorrelation function are taken in the incomplete correlation procedure and even more in the complete correlation procedure, this finite sampling error is less than $6.76/12{,}000 = 5.6 \times 10^{-4} = 0.056\%$.

This calculation is oversimplified and does not account for the very tricky $\tau \neq 0$ cases, but it does illustrate how insignificant this error is in our case. It should be noted that this sampling error occurs in both the signal noise and the quantization noise, but both are very small.

VI. EXPERIMENTAL RESULTS

The correlator described in the preceding chapters was built and successfully debugged. In its final form, the instrument has several convenience features such as input overload and output ready lights, adjustable clock, adjustable output gain, adjustable number of samples, and an output recirculate mode for oscilloscope display. Oscilloscope photographs of actual correlator calculated autocorrelation functions are shown in Figure 11. for sinusoidal, square wave, white noise, and Lorentzian noise inputs. The upper trace in each case is the autocorrelation function and the lower trace is the input signal.

The correlator-calculator system is organized in a handshaking manner with two-way communication. The correlator signals the calculator when it has completed its calculation. The calculator then clocks out the stored autocorrelation function into its memory, calculates the spectrum, plots, and prints the result. Because the autocorrelation function can be stored indefinitely and clocked out by the calculator in segments of arbitrary length, the demand on the calculator is minimal. This is particularly important for time-sharing applications instead of a dedicated calculator.

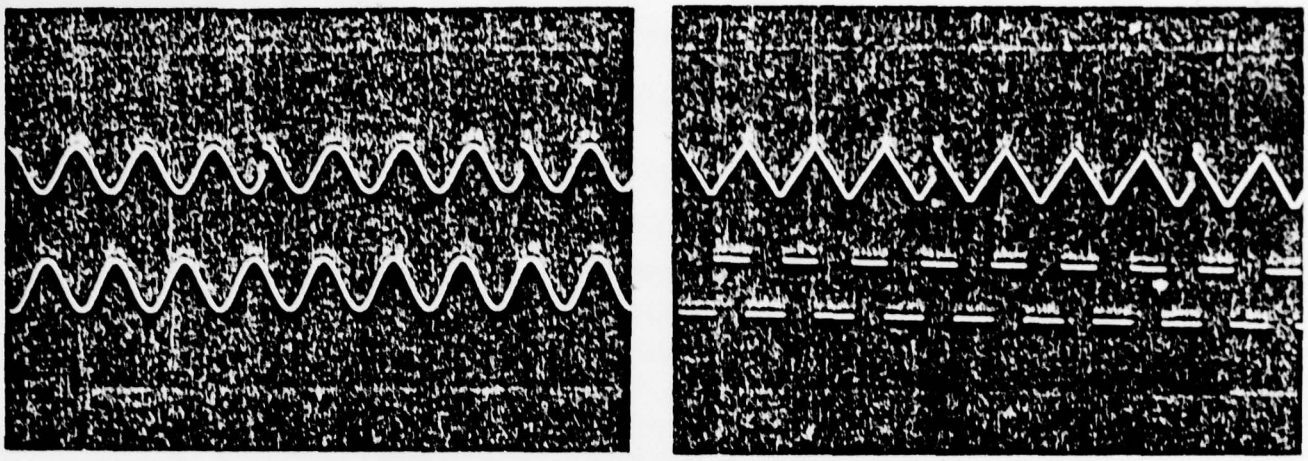

(a) (b)

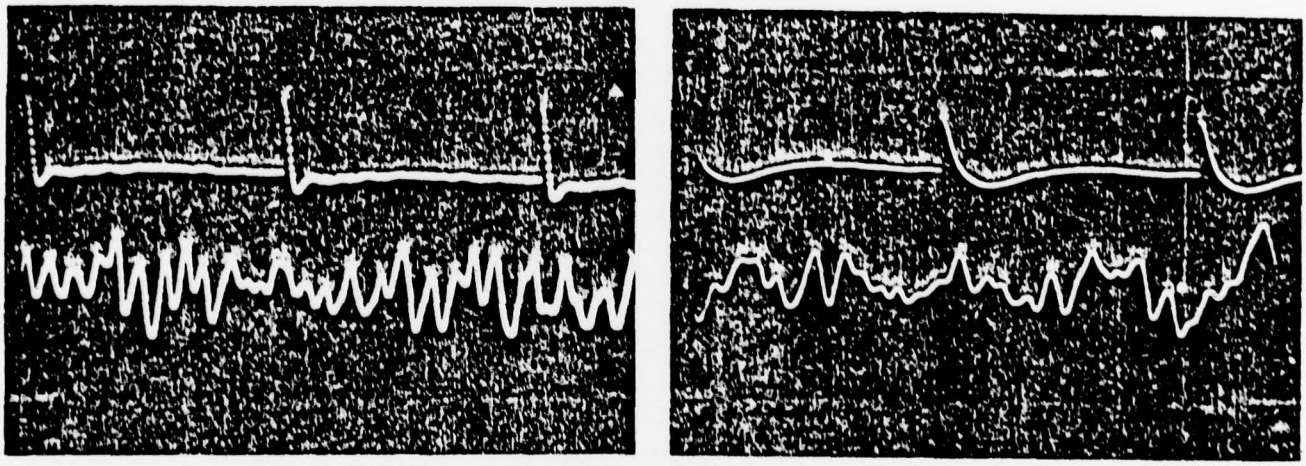

(c) (d)

Figure 11 Oscilloscope photographs of the correlator computed autocorrelation functions for (a) sinusoidal, (b) square wave, (c) white noise and (d) Lorentzian noise input signals. The input signals are shown in the lower part of each figure and the autocorrelation functions are shown in the upper part of each figure.

Figures 12 and 13 contain plots of the correlator-calculated autocorrelation function and the subsequent calculator-calculated frequency spectrum. The input signal here is Lorentzian noise with a $\frac{1}{[1+(f/f_0)^2]}$ spectrum. There is some point scatter, but a three point average shown in Figure 14 gives a smooth curve with little loss in frequency resolution. In fact, the small filter hump at about 600 Hz is still retained.

VII. CONCLUSION

We have analyzed the correlation probelm in detail, especially as it pertains to automatic noise measurement. The various errors were studied in order to design the most efficient system in terms of speed, accuracy, size, cost, and convenience. The error sources considered in this study include high frequency aliasing, low frequency resolution, A-D conversion, finite time, finite sampling, and quantization. Software calculation of the Wiener-Khintchine integral using this analysis shows that hardware correlator is most effective. The correlator uses the incomplete correlation method and four bit input resolution. This system combines the high frontend speed or broadband width and accuracy of a dedicated, hardwired correlator with the flexibility of a dedicated calculator or time-sharing computer which gives software calculated, tabulated and graphic outputs.

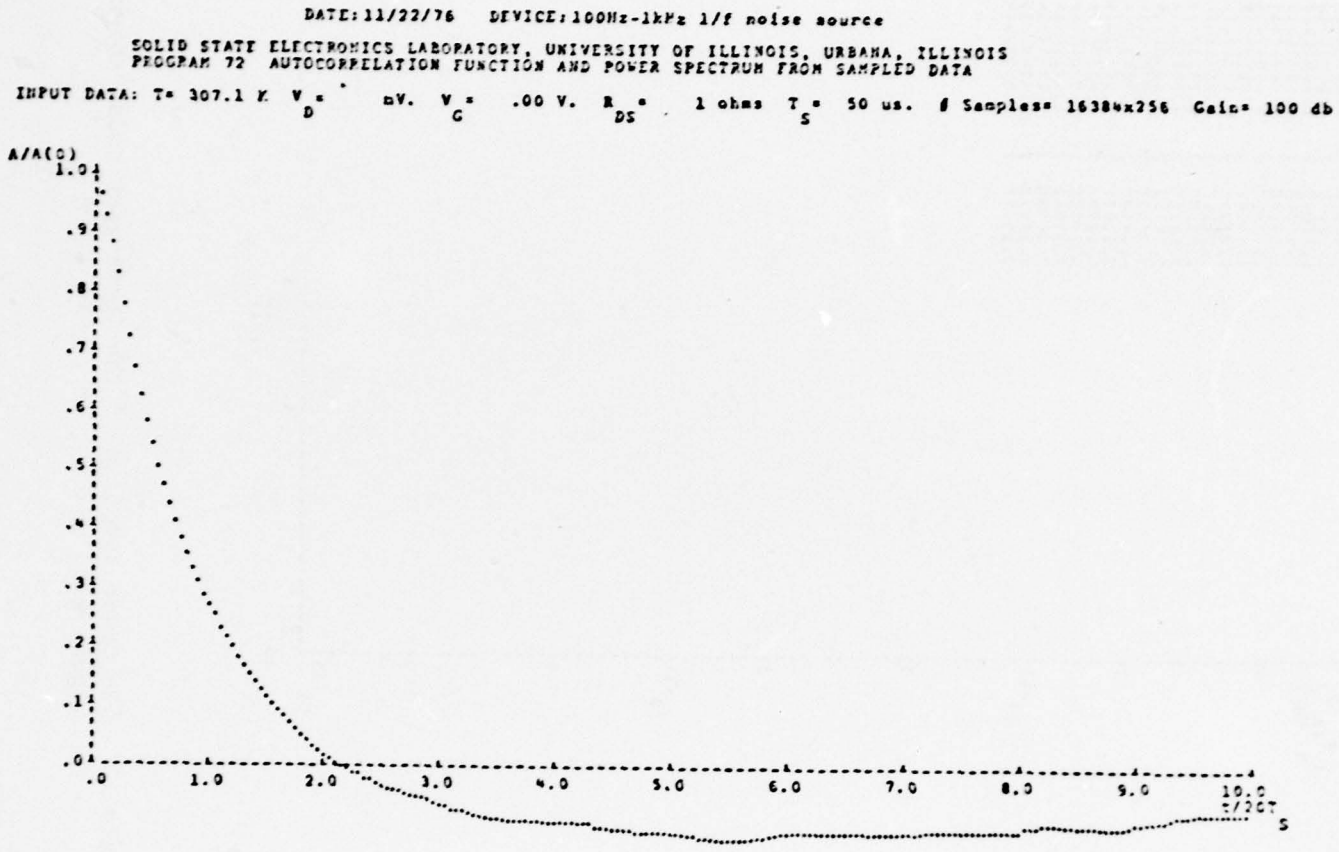

Figure 12 The autocorrelation function of a Lorentzian noise.

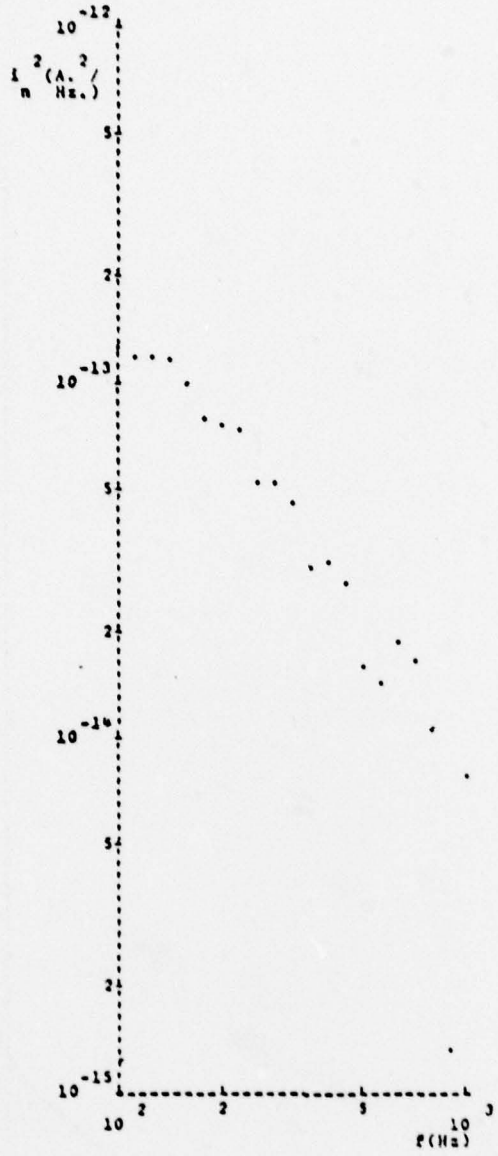

f(Hz)		i_n^2 (A.^{2}/Hz.)
1.0000E	2	1.2836E-13
1.1220E	2	1.1947E-13
1.2588E	2	1.1961E-13
1.4124E	2	1.1673E-13
1.5847E	2	1.0021E-13
1.7781E	2	8.0486E-14
1.9950E	2	7.7457E-14
2.2384E	2	7.5208E-14
2.5115E	2	5.3075E-14
2.8179E	2	5.2632E-14
3.1617E	2	4.6678E-14
3.5474E	2	3.0680E-14
3.9802E	2	3.1874E-14
4.4658E	2	2.7772E-14
5.0107E	2	1.6171E-14
5.6220E	2	1.4509E-14
6.3070E	2	1.2117E-14
7.0774E	2	1.6851E-14
7.9409E	2	1.0737E-14
8.9097E	2	1.3350E-15
9.9967E	2	8.0471E-15

Figure 13 The power spectrum of the Lorentzian noise shown in Figure 12.

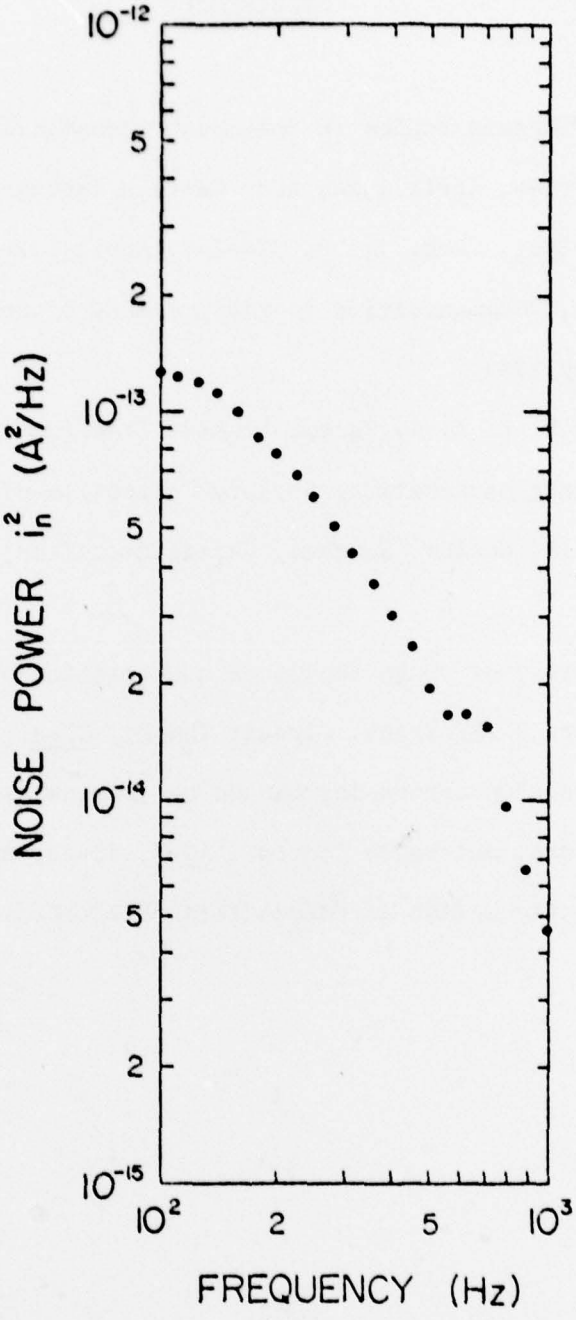

Figure 14 The three-point smoothed power spectrum of the Lorentzian noise shown in Figure 13.

REFERENCES

1. H. Nyquist, "Certain topics in telegraph transmission theory," Trans. AIEE, 47, 617-644, April 1928; and "Certain factors affecting telegraph speed," Bell Syst. Tech. J., 3, 324-346, April 1924.
2. C. E. Shannon, "Communication in the presence of noise," Proc. IRE, 37, 10-21, January 1949.
3. N. Wiener and R. E. A. C. Paley, *Fourier Transforms in the Complex Domain*, American Mathematical Society Collection of Publications, 1934.
4. A. Van der Ziel, *Noise: Sources, Characterization, Measurement*, Prentice-Hall, 1970.
5. B. Widrow, "Study of rough amplitude quantization by means of Nyquist sampling theory," IRE Trans. Circuit Theory, CT-3, 266-276, December 1956.
6. J. Katzenelson, "On errors introduced by combined sampling and quantization," IRE Trans. Automatic Control, AC-7, 58-68, April 1962.
7. P. G. Hoel, *Introduction to Mathematical Statistics*, Wiley & Sons, 1971.

MISSION
of
Rome Air Development Center

RADC plans and conducts research, exploratory and advanced development programs in command, control, and communications (C^3) activities, and in the C^3 areas of information sciences and intelligence. The principal technical mission areas are communications, electromagnetic guidance and control, surveillance of ground and aerospace objects, intelligence data collection and handling, information system technology, ionospheric propagation, solid state sciences, microwave physics and electronic reliability, maintainability and compatibility.

Printed by
United States Air Force
Hanscom AFB, Mass. 01731